Dynamical Replica Analysis of Disordered Ising Spin Systems on Finitely Connected Random Graphs

J. P. L. Hatchett,[1] I. Pérez Castillo,[2] A. C. C. Coolen,[3] and N. S. Skantzos[4]

[1]*Laboratory for Mathematical Neuroscience, RIKEN Brain Science Institute, Wako, Saitama 351-0198, Japan*
[2]*Rudolph Peirls Center for Theoretical Physics, University of Oxford, 1 Keble Road, Oxford OX1 3NP, United Kingdom*
[3]*Department of Mathematics, King's College, University of London, The Strand, London WC2R 2LS, United Kingdom*
[4]*Instituut voor Theoretische Fysica, Katholieke Universiteit Leuven, Celestijnenlaan 200, DB-3001 Leuven, Belgium*

(Received 12 April 2005; published 8 September 2005)

We study the dynamics of macroscopic observables such as the magnetization and the energy per degree of freedom in Ising spin models on random graphs of finite connectivity, with random bonds and/or heterogeneous degree distributions. To do so, we generalize existing versions of dynamical replica theory and cavity field techniques to systems with strongly disordered and locally treelike interactions. We illustrate our results via application to, e.g., $\pm J$ spin glasses on random graphs and of the overlap in finite connectivity Sourlas codes. All results are tested against Monte Carlo simulations.

DOI: 10.1103/PhysRevLett.95.117204 PACS numbers: 75.10.Nr, 05.20.−y, 64.60.Cn

Recent years have witnessed a surge of interest in the study of finitely connected disordered spin systems. From a physical point of view, despite their lack of a realistic geometry and their mean-field nature, the finite number of neighbors per spin in such models does give rise to a nontrivial local geometry and ensuing artifacts. Here we simply regard the random bond finite connectivity Ising spin system as the archetypal interacting particle model on a disordered random graph. Such models are important in the understanding of algorithmic complexity in theoretical computer science [1–3], and also underlie recent theoretical advances for an important class of error correcting codes [4–6]. It has been shown that the tuning of the degree distribution and/or the connectivity strengths in complex networks can lead to atypical mean-field critical phenomena [7–9], and they are now increasingly and fruitfully used for modeling neural, social, Internet, gene regulatory, and proteomics networks [10–13]. While our quantitative understanding of the equilibrium properties of these systems is quite advanced (see, e.g., [14,15]), the tools available for studying their nonequilibrium behavior are comparatively poor. There has been some progress in applying the path integral techniques of [16] to spherical and related models [17], and to Ising models with parallel spin updating [18,19]. Generalizing such approaches to Ising spin models with Glauber-type dynamics requires the treatment of nontrivial functional order parameters that have, as yet, not been adequately controlled. An alternative approach, which we follow here, is to generalize the techniques of dynamical replica theory [20], together with the cavity field concept, to finitely connected disordered spin systems. This approach has already proven fruitful for weakly disordered dilute ferromagnets [21] where each spin is effectively in an identical environment. In this Letter, in contrast, we study the dynamics of strongly disordered versions of finitely connected Ising systems, where each spin is in a highly *heterogeneous* environment, due to the presence of either random bonds or nodes with variable degrees.

Our model consists of N Ising spins $s_i \in \{-1, 1\}$, $i = 1, \ldots, N$, whose mutual interactions are characterized by a range-free symmetric adjacency matrix with entries $c_{ij} \in \{0, 1\}$ and symmetric bonds $J_{ij} \in \mathrm{IR}$. We define $c_{ii} = 0$, and draw the bond strengths J_{ij} independently from some distribution $Q(J)$. The probability of finding any state $\mathbf{s} \equiv (s_1, \ldots, s_N)$ of the system at time t is given by the measure $p_t(\mathbf{s})$, which evolves as the spins align asynchronously and stochastically to their local fields, according to a Glauber dynamics in the form of the master equation

$$\frac{d}{dt} p_t(\mathbf{s}) = \sum_{k=1}^{N} [p_t(F_k\mathbf{s}) w_k(F_k\mathbf{s}) - p_t(\mathbf{s}) w_k(\mathbf{s})], \quad (1)$$

where $F_k\mathbf{s} \equiv (s_1, \ldots, -s_k, \ldots, s_N)$ is the kth spin-flip operator and the transition rates $w_k(\mathbf{s})$ have the standard form

$$w_k(\mathbf{s}) \equiv \tfrac{1}{2}\{1 - s_k \tanh[\beta h_k(\mathbf{s})]\} \quad (2)$$

with the local fields $h_i(\mathbf{s}) \equiv \Sigma_{j \neq i} c_{ij} J_{ij} s_j + \theta$. This process evolves toward equilibrium, with the Boltzmann measure and with Hamiltonian

$$H(\mathbf{s}) = -\sum_{i<j} s_i c_{ij} J_{ij} s_j - \theta \sum_i s_i. \quad (3)$$

Following the procedure outlined for fully connected systems [20], we consider the evolution of two macroscopic observables, the magnetization $m(\mathbf{s}) = N^{-1}\Sigma_i s_i$, and the internal energy $e(\mathbf{s}) = -N^{-1}\Sigma_{i<j} c_{ij} J_{ij} s_i s_j$. We abbreviate $\mathbf{\Omega} = (m, e)$. One easily derives a Kramers-Moyal (KM) expansion for their probability density $\mathcal{P}_t(\mathbf{\Omega}) = \Sigma_{\mathbf{s}} p_t(\mathbf{s}) \delta[\mathbf{\Omega} - \mathbf{\Omega}(\mathbf{s})]$; see, e.g., [22]. On finite times one finds that only the first (so-called Liouville) term in the KM expansion survives the thermodynamic limit, so the observables (m, e) evolve deterministically, i.e., $\lim_{N\to\infty} P_t(\mathbf{\Omega}) = \delta[\mathbf{\Omega} - \mathbf{\Omega}_t]$ with

$$\frac{d}{dt}\mathbf{\Omega}_t = \lim_{N\to\infty} \sum_{\mathbf{s}} p_t(\mathbf{s}|\mathbf{\Omega}_t) \sum_i w_i(\mathbf{s})[\mathbf{\Omega}(F_i\mathbf{s}) - \mathbf{\Omega}(\mathbf{s})], \quad (4)$$

$$p_t(\mathbf{s}|\mathbf{\Omega}) = \frac{p_t(\mathbf{s})\delta[\mathbf{\Omega} - \mathbf{\Omega}(\mathbf{s})]}{\sum_{\mathbf{s}'} p_t(\mathbf{s}')\delta[\mathbf{\Omega} - \mathbf{\Omega}(\mathbf{s}')]}. \quad (5)$$

Equation (4) still involves the conditional microscopic distribution $p_t(\mathbf{s}|\mathbf{\Omega})$. To proceed, we follow [20]: (i) we assume that the observables $\mathbf{\Omega}$ are self-averaging at all times (which one expects to be true), and (ii) we approximate the microscopic measure $p_t(\mathbf{s}|\mathbf{\Omega})$ by the maximum entropy distribution given the condition that the macroscopic observables take the value $\mathbf{\Omega}$. These assumptions imply that our observables evolve according to

$$\frac{d}{dt}m_t = -m_t + \int dh\, \mathcal{D}(h|m_t, e_t)\tanh(\beta h), \quad (6)$$

$$\frac{d}{dt}e_t = -2e_t - \int dh\, \mathcal{D}(h|m_t, e_t) h \tanh(\beta h). \quad (7)$$

Here $\mathcal{D}(h|m_t, e_t)$ denotes the asymptotic distribution of local fields in a system with magnetization m_t and energy e_t,

$$\mathcal{D}(h|e_t, m_t) = \lim_{N\to\infty} \frac{1}{N} \sum_{i=1}^{N} [\langle \delta[h - h_i(\mathbf{s})]\rangle_{m_t,e_t}]_{\text{dis}}, \quad (8)$$

where the average $\langle\cdots\rangle_{m_t,e_t}$ is over the maximum entropy distribution given the values of the observables, viz., over

$$p(\mathbf{s}|m_t, e_t) \equiv \frac{\delta[m_t - m(\mathbf{s})]\delta[e_t - e(\mathbf{s})]}{\sum_{\mathbf{s}'}\delta[m_t - m(\mathbf{s}')]\delta[e_t - e(\mathbf{s}')]} \quad (9)$$

and $[\cdots]_{\text{dis}}$ is over the disorder (the realization of the random graph and bonds).

The relatively simple solution in [21] can be understood within this framework. Since all sites were identical, there was just a single cavity field. Hence the distribution of local fields was uniform across sites and could be given explicitly in terms of the observables.

The field distribution $\mathcal{D}(h|m_t, e_t)$ is readily calculated, even in the presence of bond or degree disorder, either via the replica method or via the cavity approach for dilute systems [14] (in the microcanonical or the canonical framework, respectively) [23]. Here the resulting equations from either approach are the same. They correspond to the maximum entropy distribution, given (m_t, e_t), which equals the equilibrium distribution of a system with Hamiltonian (3) but with a pseudo inverse temperature $\hat{\beta}$ and pseudo external field $\hat{\theta}/\hat{\beta}$. These act as Lagrange parameters, enforcing the condition that the equilibrium distribution gives the required values of (m_t, e_t). The prefix "pseudo" indicates that these parameters need not be physical: there could be states (m_t, e_t) for which $\hat{\beta}$ is negative. More specifically, the replica method allows us to perform the disorder average in (8), using the identity

$$\left[\sum_{\mathbf{s}} \delta[h - h_i(\mathbf{s})]p(\mathbf{s}|m_t, e_t)\right]_{\text{dis}} = \lim_{n\to 0} \sum_{\mathbf{s}^1,\ldots,\mathbf{s}^n} \left[\delta[h - h_i(\mathbf{s}^1)] \prod_{\alpha=1}^{n} (\delta[m_t - m(\mathbf{s}^\alpha)]\delta[e_t - e(\mathbf{s}^\alpha)])\right]_{\text{dis}} \quad (10)$$

followed by making the so-called replica symmetric (RS) ansatz for the emerging (dynamical) order parameters. Within the cavity formalism we can work either with the ensemble or with a particular realization of the disorder. The latter tends to be numerically simpler, due to the inherent (finite size) noise in population dynamics, which limits the accuracy with which the Lagrange parameters can be calculated. Working in areas of phase space where replica symmetry is expected to be exact and where our belief propagation algorithm [24] converged, it was possible to find the Lagrange parameters to high precision (fixed points of the belief propagation algorithm describe minima of the Bethe free energy [25]). For large graph sizes the differences between results for graph realization and the ensemble average ought to vanish.

The resulting numerical algorithm is as follows. At any given point in time we know the instantaneous values (m_t, e_t) of our observables. We then run a belief propagation algorithm [24] on our graph, for a given pair of Lagrange parameters $(\hat{\beta}, \hat{\theta})$ which act as inverse temperature and external field; once the belief propagation has converged, we can measure $[m_t(\hat{\beta}, \hat{\theta}), e_t(\hat{\beta}, \hat{\theta})]$. We now vary the Lagrange parameters and repeat the above until we satisfy the condition

$$m_t = m_t(\hat{\beta}, \hat{\theta}), \qquad e_t = e_t(\hat{\beta}, \hat{\theta}). \quad (11)$$

Finally we use the cavity fields generated with the correct values of $(\hat{\beta}, \hat{\theta})$ to give the local field distribution within our graph, with which we can evaluate the force terms in (6) and (7). We should emphasize that the status of the above procedure is only that of a numerical tool with which to solve the dynamical order parameters from the closed equations provided by the dynamical replica theory, and hence generate the theoretical predictions for the dynamics of an infinitely large system. It should not be confused with microscopic Monte Carlo (MC) simulations of the underlying spin system, as, e.g., employed below.

In Fig. 1 we compare the results of our analysis with MC simulations for a $\pm J$ spin glass on a 3-regular graph. We sampled our graph uniformly from all connected graphs where each site has exactly three neighbors and each bond is drawn independently from $Q(J) = \eta\delta(J - 1) + (1 - \eta)\delta(J + 1)$. All MC simulations were carried out with a system size of $N = 10\,000$ and were run on the same realization of the graph as the cavity field calculations. We see an excellent correspondence between theory and MC simulations. We have taken η to be relatively large (predominance of ferromagnetic bonds), since we did not wish to move into a region where belief propagation would not converge, a condition one expects to be closely related to instability in the de Almeida–Thouless (AT) sense [26,27]. In such regions it is no longer possible to use

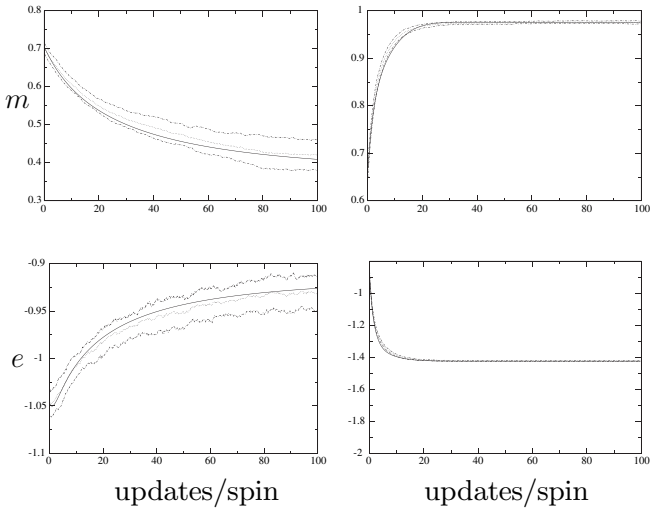

FIG. 1. Evolution of the magnetization m (top) and the energy e (bottom), for Ising spins on a 3-regular random graph with random bonds, and with time measured in units of updates per spin. Bond distribution: $Q(J) = \eta\delta(J-1) + (1-\eta)\delta(J+1)$. Solid lines denote the theoretical predictions. Dotted lines represent the MC simulation data (system size $N = 10\,000$ and averaged over 50 runs), with dot-dashed lines giving the averages ± 1 standard deviation. Left: $\eta = 0.95$ and $\beta = 0.65$. Right: $\eta = 0.97$ and $\beta = 1.2$.

belief propagation for accurately evaluating the Lagrange parameters $\hat{\beta}$ and $\hat{\theta}$.

It is also of interest to note in Fig. 2 that the evolution of the pseudo inverse temperature need not be monotonic. Assuming that the location of the AT line [26] is similar to that of the fully connected case, i.e., that it goes continuously from the zero-temperature instability ($T = 0$, $\eta = \frac{11}{12}$) [28,29] to the triple point ($T \approx 1.13$, $\eta \approx 0.85$), as in [27], one could have a situation where starting from a RS phase, the parameters (β, η) could be chosen such that the final equilibrium phase was also RS, but where the dynamics takes the system through a regime of phase space where in equilibrium one would find replica symmetry breaking. Since there the belief propagation (or any other replica symmetric) algorithm would not converge in a time of $\mathcal{O}(N)$, the algorithm would become stuck *en route* to RS equilibrium.

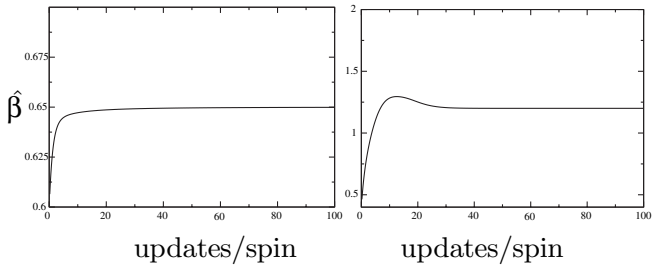

FIG. 2. Evolution of the pseudo inverse temperature Lagrange parameter $\hat{\beta}$ for the experiments shown in Fig. 1. Clearly, the relaxation of $\hat{\beta}$ need not be monotonic.

In Fig. 3 we examine the order parameter flow in ferromagnetic random graphs with average connectivity 2 and 3, respectively. Here each bond is independently defined to be present ($c_{ij} = 1$) with probability c/N, where c is the average connectivity, leading to a graph with a Poisson degree distribution (or Erdös-Rényi graph). In these systems the inhomogeneity of the local environment of the spins is no longer caused by bond disorder, but by nonuniform connectivity. The agreement between theory and MC simulations in the case $c = 2$ is significantly worse than that in the other examples presented. The maximum entropy measure appears to be a much less accurate approximation of the true microscopic distribution, which tells us that the system evolves through statistically atypical microscopic states, and predicts a relaxation of the order parameters that is far too quick. This would appear to be related to the increased heterogeneity associated with lower temperatures and lower average connectivity. However, plotting in the m-e plane we see that the predicted direction of the flow is still quite reasonable.

As a final example, we turn to the decoding dynamics of finite connectivity Sourlas codes [4,5,30] with 2-body interactions, which can easily be studied within the current

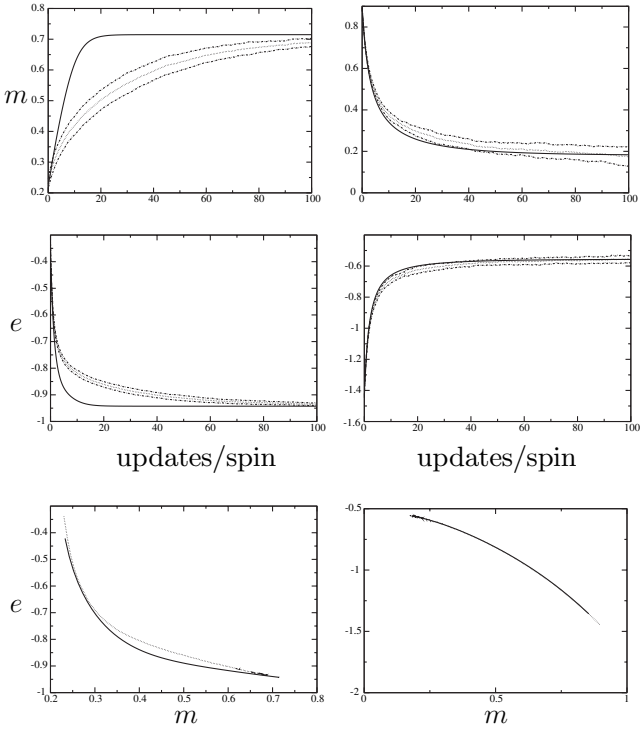

FIG. 3. Evolution of the magnetization m (top) and the energy e (bottom), for Ising spins on a Poisson random graph (of average connectivity c) with ferromagnetic bonds $J_{ij} = 1$, and with time measured in units of updates per spin (top 4 graphs) or flow in m-e place (bottom 2 graphs). Solid lines denote the theoretical predictions. Dotted lines represent the MC simulation data (system size $N = 10\,000$ and averaged over 50 runs), with dot-dashed lines giving the averages ± 1 standard deviation. Left: $c = 2$ and $T = 0.75$. Right: $c = 3$ and $T = 2.8$.

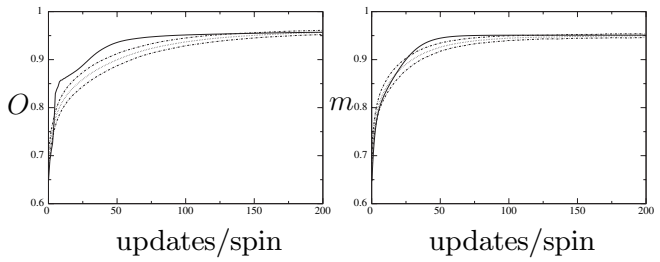

FIG. 4. Decoding dynamics of the overlap O (left) and the magnetization m (right), for a 2-body interaction and rate $\frac{2}{3}$ Sourlas error correcting code. Solid lines denote the theoretical predictions. Dotted lines represent the MC simulation data (system size $N = 10\,000$ and averaged over 50 runs), with dot-dashed lines giving the averages ± 1 standard deviation. The temperature is Nishimori's temperature for the flip probability (error rate) 0.04.

framework. In particular, in Fig. 4 we consider the case of an unbiased source broadcasting through a binary symmetric channel with flip probability 0.04 and rate $\frac{2}{3}$ (the channel capacity as given by Shannon's theorem is 0.76...). If a message $(\xi_1, \ldots, \xi_N)$ is sent across this channel, and our estimator for this message (given the corrupt channel) is given by $(\hat{\xi}_1, \ldots, \hat{\xi}_N)$, then a natural performance measure is the overlap between the message sent and the decoded message, $O = N^{-1}\Sigma_i \xi_i \hat{\xi}_i$. We decode at Nishimori's temperature, which is the temperature maximizing this particular overlap observable [31] (the so-called maximizer of posterior marginals). Although qualitatively correct, the predicted relaxation of the order parameters is again too fast compared with the MC simulation data.

In this Letter we have presented a relatively simple dynamical formalism, combining dynamical replica theory with the cavity method, to be used as a systematic approximation tool with which to understand the main features of the dynamics of dilute and disordered spin systems. We regard the wide applicability of the method as its strength. From the various applications presented here we see that our approach performs excellently in some cases, but relaxes too quickly in others, compared with numerical MC simulations. This is not unexpected [20]. However, as with the original dynamical replica theory, there is scope for increasing the order parameter set [20,21], which should improve its accuracy systematically, albeit at a numerical cost. At present our method requires the convergence of belief propagation. It would therefore seem that breaking replica symmetry within this formalism will be nontrivial to implement, even though theoretically it is a straightforward generalization. For a single experiment we here run belief propagation $\mathcal{O}(10^5)$ times; running a finite temperature one step replica symmetry breaking scheme that many times would be computationally extremely demanding without further approximations.

We warmly thank M. Okada, B. Wemmenhove, and T. Nikoletopoulos for helpful discussions and comments.

[1] M. Mézard, G. Parisi, and R. Zecchina, Science **297**, 812 (2002).
[2] R. Monasson, R. Zecchina, S. Kirkpatrick, B. Selman, and L. Troyansky, Nature (London) **400**, 133 (1999).
[3] O. C. Martin, R. Monasson, and R. Zecchina, Theor. Comput. Sci. **265**, 3 (2001).
[4] Y. Kabashima and D. Saad, Europhys. Lett. **45**, 97 (1999).
[5] I. Kanter and D. Saad, Phys. Rev. E **61**, 2137 (2000).
[6] Y. Kabashima and D. Saad, J. Phys. A **37**, R1 (2004).
[7] M. Leone, A. Vazquez, A. Vespignani, and R. Zecchina, Eur. Phys. J. B **28**, 191 (2002).
[8] A. V. Goltsev, S. N. Dorogovtsev, and J. F. F. Mendes, Phys. Rev. E **67**, 026123 (2003).
[9] C. V. Giuraniuc, J. P. L. Hatchett, J. O. Indekeu, M. Leone, I. Pérez Castillo, B. Van Schaeybroeck, and C. Vanderzande, cond-mat/0408399 [Phys. Rev. Lett. (to be published)].
[10] B. Wemmenhove and A. C. C. Coolen, J. Phys. A **36**, 9617 (2003); I. Pérez Castillo, B. Wemmenhove, J. P. L. Hatchett, A. C. C. Coolen, N. S. Skantzos, and T. Nikoletopoulos, J. Phys. A **37**, 8789 (2004).
[11] S. Galam, Y. Gefen, and Y. Shapir, Math. J. Socio. **9**, 1 (1982).
[12] L. Correale, M. Leone, A. Pagnani, M. Weigt, and R. Zecchina, cond-mat 0412443.
[13] S. N. Dorogovtsev and J. F. F. Mendes, *Evolution of Networks* (Oxford University Press, Oxford, 2001).
[14] M. Mézard and G. Parisi, Eur. Phys. J. B **20**, 217 (2001).
[15] M. Mézard and G. Parisi, J. Stat. Phys. **111**, 1 (2003).
[16] C. DeDominicis, Phys. Rev. B **18**, 4913 (1978).
[17] G. Semerjian and L. Cugliandolo, Europhys. Lett. **61**, 247 (2003).
[18] J. P. L. Hatchett, B. Wemmenhove, I. Pérez Castillo, T. Nikoletopoulos, N. S. Skantzos, and A. C. C. Coolen, J. Phys. A **37**, 6201 (2004).
[19] J. P. L. Hatchett, in *Science of Complex Networks: From Biology to the Internet and WWW, Proceedings of CNET 2004*, edited by J. F. F. Mendes *et al.*, AIP Conf. Proc. No. 776 (AIP, Melville, NY, 2005).
[20] A. C. C. Coolen and D. Sherrington, J. Phys. A **27**, 7687 (1994); S. N. Laughton, A. C. C. Coolen, and D. Sherrington, J. Phys. A **29**, 763 (1996).
[21] G. Semerjian and M. Weigt, J. Phys. A **37**, 5525 (2004).
[22] N. G. Van Kampen, *Stochastic Processes in Physics and Chemistry* (Elsevier, New York, 1992).
[23] Although the replica approach is more general since it does not require the existence of a Hamiltonian, it also allows for the study of systems without detailed balance.
[24] J. Pearl, *Probabilistic Reasoning in Intelligent Systems: Networks of Plausible Inference* (Morgan Kaufmann, San Francisco, CA, 1988).
[25] J. S. Yedidia, W. T. Freeman, and Y. Weiss, Neural Inf. Process. Syst. **13**, 689 (2000).
[26] J. R. L. deAlmeida and D. J. Thouless, J. Phys. A **11**, 983 (1978).
[27] Y. Kabashima, J. Phys. Soc. Jpn. **72**, 1645 (2003).
[28] C. Kwon and D. J. Thouless, Phys. Rev. B **37**, 7649 (1988).
[29] T. Castellani and F. Ricci-Tersenghi, cond-mat/0403053.
[30] T. Ozeki and M. Okada, Prog. Theor. Phys. Suppl. (to be published).
[31] P. Rujan, Phys. Rev. Lett. **70**, 2968 (1993).